RESEARCH

Heat stress in South America over the last four decades: a bioclimatic analysis

Vitor F. V. V. Miranda[1,2,3] · Djacinto Monteiro dos Santos[1] · Leonardo F. Peres[1] · Coral Salvador[4,5,6] · Raquel Nieto[4] · Gabriela V. Müller[7,8] · Dirk Thielen[9] · Renata Libonati[1,10,11]

Abstract
The observed continuous rise in the frequency of extreme heat events in South America (SA) poses a serious challenge for public health. However, there is a lack on the understanding of the large-scale and long-term variability and trends of thermal stress in this continent. Accordingly, here we developed the first comprehensive bioclimatology of thermal stress over SA during the past four decades. Consecutive heat stress hours were analyzed using the Universal Thermal Climate Index (UTCI) from ERA5-HEAT reanalysis according to the Köppen–Geiger climate classification and also focusing on the 31 most populated cities of SA. Results show an inland/coastline contrast and a marked latitudinal northward increase in the number of hours under heat stress. Heat stress hotspots are located mostly around the Amazon, northern and central parts of SA with 26–35% of the hours between 1979 and 2020 under strong heat stress. The annual number of hours within heat stress increased significantly between 1979 and 2020, varying from + 1.16 h/year to + 8.25 h/year depending on the Köppen–Geiger class. The past 20 years (2000 forward) presented not only more consecutive hours under heat stress than the previous two decades in all the analyzed cities, but also a higher persistence of such conditions. The bioclimatology of thermal stress developed here may provide important guidelines to decision-makers for exploring adaptation strategies to increase societal resilience.

✉ Renata Libonati
renata.libonati@igeo.ufrj.br

1   Departamento de Meteorologia, Universidade Federal do Rio de Janeiro, Rio de Janeiro 21941-916, Brazil

2   Earth Observation Unit, Portuguese Institute of Sea and Atmosphere, 1749-077 Lisboa, Portugal

3   Department of Earth Physics and Thermodynamics, Universitat de Valencia, 46100 Valencia, Spain

4   Centro de Investigación Mariña, Environmental Physics Laboratory (EPhysLab), Universidade de Vigo, Ourense, Spain

5   Institute of Social and Preventive Medicine (ISPM), University of Bern, Bern, Switzerland

6   Oeschger Center for Climate Change Research, University of Bern, Bern, Switzerland

7   Centro de Variabilidad y Cambio Climático (CEVARCAM), Facultad de Ingeniería y Ciencias Hídricas (FICH), Universidad Nacional del Litoral (UNL), Ciudad Universitaria, Santa Fe, Argentina

8   Consejo Nacional de Investigaciones Científicas y Técnicas (CONICET), Santa Fe, Argentina

9   Instituto Venezolano de Investigaciones Científicas, Caracas, Venezuela

10 Forest Research Centre, School of Agriculture, University of Lisbon, 1349-017 Lisbon, Portugal

11 Instituto Dom Luiz, Faculdade de Ciências, Universidade de Lisboa, 1749-016 Lisbon, Portugal

1 Introduction

According to the sixth assessment report of IPCC (Seneviratne et al. 2021), human-induced global warming has already caused multiple changes in the climate system, such as the increase in the intensity, duration, and frequency of extreme heat events. Climate models project a continuous rise in the frequency of these extremes in the following decades (Power and Delage 2019), exposing around half of the world's human population to excessively hot temperatures (Mora et al. 2017). Until the end of this century, depending on the rates of warming and population growth, 1 to 3 billion people are expected to live in regions outside the interval of climatic conditions suitable for humans (Xu et al. 2020). In particular, heat waves (HW) have been observed to increase over the past four decades around the globe with faster rates in tropical and polar regions (Zhang et al. 2022). In this context, studies using different methods and datasets have identified positive trends in extreme hot events in distinct regions of South America (SA) over the past decades (Regoto et al. 2021; Rusticucci et al. 2016; Geirinhas et al. 2018; Libonati et al. 2022b; Costa et al. (2022). Moreover, climate model outputs suggest a continuous rise in the frequency of extreme hot events in the coming decades in SA (Feron et al. 2019). By the end of the XXI century, several SA countries are likely to experience higher levels of heat-related health stress due to the increased severity of natural hazards and ongoing population growth (Hagen et al. 2022). A global average temperature rise of 1.5 °C to 3 °C is expected to increase population exposure to heat events from 2 to 6 million and from 1 to 4 million people on the southeastern and west coast of SA, respectively (Liu et al. 2021), with negative effects on society and major negative impacts on the public health sector (Perkins-Kirkpatrick and Lewis 2020; Vicedo-Cabrera et al. 2021).

Heat affects human health both directly and indirectly. Regarding direct effects, prolonged exposure to extreme temperatures can alter human thermoregulation (Ahima 2020), which helps the body to maintain the internal temperature within specific boundaries (Cheshire 2016). Heat stress occurs when the human thermoregulatory mechanism is disrupted and the body produces more heat than it dissipates, leading body temperature and heart rate to increase (Cramer and Jay 2016). This imbalance of internal energy in the human body can lead to discomfort, fainting, and increased risk of morbidity and mortality (Di Napoli et al. 2019). Heat-related disorders mainly include cardiovascular, respiratory, and kidney diseases (Wellenius et al. 2017). However, excessive heat also influences mental health and suicide rates, as well as work-related injuries and illnesses, and human cognitive performance (Florido Ngu et al. 2021; Varghese et al. 2019; Hancock and Vasmatzidis

2003). Elevated temperatures have also been associated with a higher risk of preterm birth, low birth weight, and stillbirth (Barreca and Schaller 2020; Libonati et al. 2022a). Regarding indirect effects, hot temperatures are often linked with dry conditions and high vegetation flammability, thus favoring the occurrence of wildfires, and consequently the decrease of air quality and increase of hospitalization risk due to respiratory diseases (Libonati et al. 2022b; Shaposhnikov et al. 2014; Machado-Silva et al. 2020). There is also evidence linking increased temperatures with changes in the incidence of vector-, water-, and food-borne infectious diseases, such as dengue outbreaks in tropical regions (Cheng et al. 2020). The effects of extreme temperature on human population depend on individual characteristics such as age, gender, and pre-existing diseases, but also on the socioeconomic and political situation (Romanello et al. 2021). Vulnerable groups such as the elderly, children, pregnant, the poorest, and those suffering from cardiovascular, respiratory, or diabetic diseases are more affected by prolonged extreme heat (Guo et al. 2017; Patz et al. 2005).

Urban populations are the most exposed to extreme heat because of the urban heat island effect. In particular, almost 80% of people in Latin America live in cities (WHO 2017) and most SA countries are considered highly vulnerable due to their growing population, fragile public health systems, and poor sanitary and education conditions (Herold et al. 2017). Human exposure to extremely hot temperatures has been linked to an increased risk of death and hospitalization in Latin America (Kephart et al. 2022), namely in Argentina (García-Witulski and Rabass 2021), Brazil (Geirinhas et al. 2019; Libonati et al. 2022a), Chile (Romero-Lankao et al. 2013), and Colombia (Romero-Lankao et al. 2013). Recently, a comprehensive global analysis, including 47 cities in 6 countries of SA (Uruguay, Peru, Brazil, Argentina, Colombia, and Ecuador) showed that the mortality risk during hot events was greater under fast and large temperature fluctuation (Wu et al. 2022). Another recent study conducted across 732 locations in 43 countries (eight of which are in SA), estimated that 37% of heat-related mortality in the warm season was attributable to human-induced climate change during the 1991–2018 period. Differences were observed among regions, with the largest attributions found in several countries in Central and South America, besides locations in Asia (Vicedo-Cabrera et al. 2021).

For a better understanding of thermal stress and its adverse health effects, the Universal Thermal Climate Index (UTCI; Jendritzky et al. 2012; Bröde et al. 2013) was developed in 2009, in the framework of COST (European Cooperation in Scientific and Technical Research) Action 730 (Jendritzky et al. 2007). The index was developed to quantify the thermophysiological effects of the meteorological conditions on people, thus describing how the human

body reacts to thermal variables (e.g. air temperature, wind speed, relative humidity, and radiation fluxes) (Di Napoli et al. 2021b). Therefore, the UTCI can be applied in research initiatives aiming at climate change mitigation and to understand the bioclimatology of different regions (Krüger 2021). A historical global gridded dataset of UTCI, named ERA5-HEAT (Human thErmAl comforT) was recently developed to represent the spatial distribution of human thermal comfort (Di Napoli et al. 2021b). ERA5-HEAT uses climate variables from ERA5 reanalysis (Hersbach et al. 2020) that match in-situ observations quite well and are thus suitable for temperature-related health risk estimates (Mistry et al. 2022). In this context, Antonescu et al. (2021) recently developed a bioclimatology of thermal stress in Europe from 1979 to 2019 using the UTCI derived from ERA5-HEAT. However, few studies globally analyzed thermal comfort indexes such as UTCI and heat stress based on gridded data (Di Napoli et al. 2018; Antonescu et al. 2021). In the case of SA, the overwhelming majority of studies using UTCI rely on single-point analysis using in-situ data and are limited to a few regions in Brazil, namely the main cities (Silva and Hirashima 2021).

Accordingly, there is a lack of large-scale and long-term studies analyzing thermal stress variability and trends over SA. Our work aims to fill this gap by analyzing the patterns in consecutive heat stress hours using the UTCI from ERA5-HEAT reanalysis focusing on the 31 most populated cities of SA during the past four decades (1979–2020). Here we developed a bioclimatology of thermal stress of SA by assigning the UTCI to each bioclimatic zone based on the 1-km Köppen–Geiger climatology for the recent period (1980–2016, Peel et al. 2007; Beck et al. 2018). To our knowledge, this is the first-ever work using gridded data to analyze heat stress in SA.

2 Materials and methods

2.1 ERA5-HEAT-derived UTCI data

The ERA5-HEAT v1.0 gridded reanalysis, containing the hourly UTCI dataset from 1979 to 2020 at $0.25° \times 0.25°$ resolution corresponding to SA, was downloaded from the Copernicus Climate Change Service (https://cds.climate.copernicus.eu, C3S, 2020). ERA5-HEAT is derived from ERA5 reanalysis using hourly climate variables (Hersbach et al. 2020), namely air (Ta) and dew point (Td) temperatures at 2 m above ground level (agl), wind speed at 10 m agl (va), and solar and thermal radiation at the Earth's surface. Additionally, relative humidity (RH) and the cosine of the solar zenith angle (cosθ0) are computed and used as input to the model. RH is derived from the Clausius-Clapeyron relation

using Ta and Td, and cosθ0 is obtained from the solar declination angle, geographic latitude, and the hour angle in local solar time, as detailed in Di Napoli et al. (2021b).
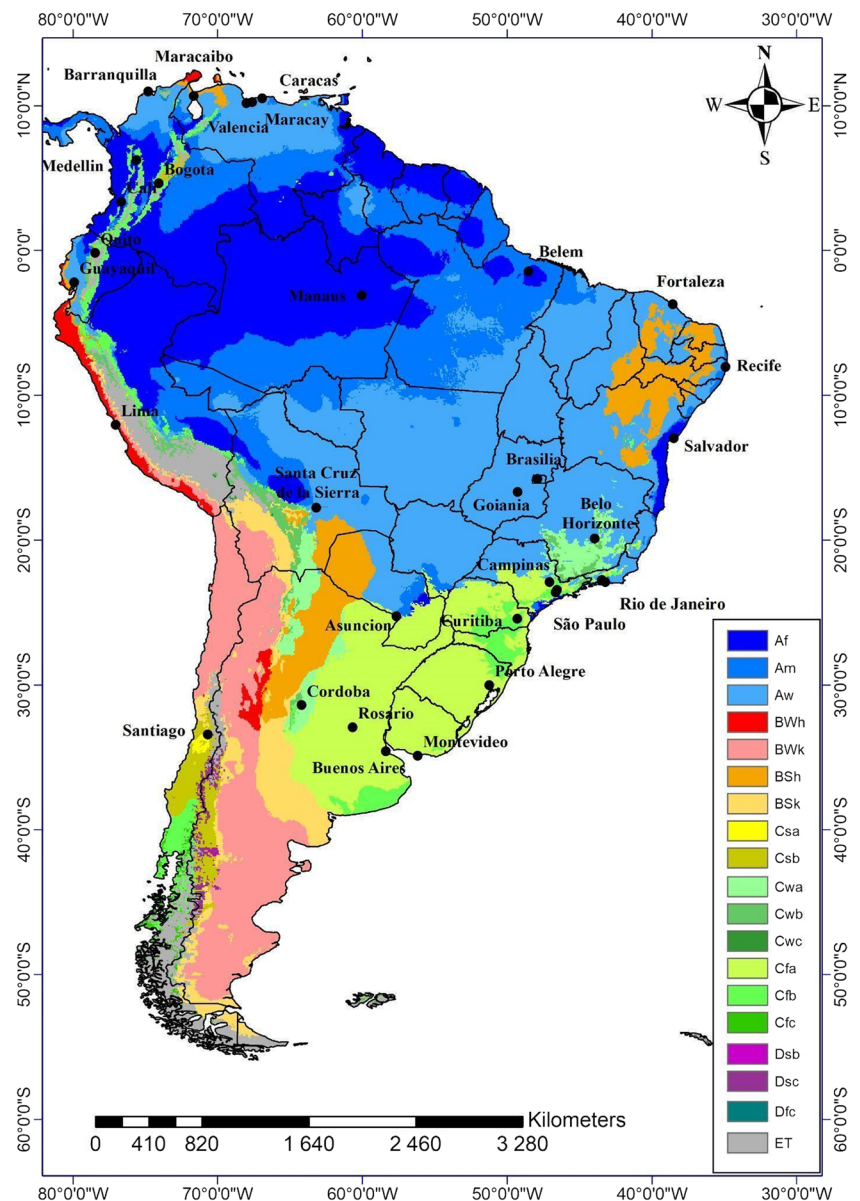
The process described by Di Napoli et al. (2021b) first computes the Mean Radiant Temperature (MRT). MRT is a critical physical quantity representing how human beings experience radiation. It summarizes the complex radiant outdoor environment effects on the human body into a unique and uniform temperature which would result in the same net radiation energy exchange of the actual environment (Kántor and Unger 2011). The first step to compute the MRT is to retrieve the surface projection factor (Fp), which represents the portion of the body surface exposed to direct solar radiation. Fp is computed from the solar elevation angle (γ) as defined by Jendritzky (1990), where γ is the complementary angle to the solar zenith angle (in degrees). The second step is to compute the direct and diffuse components of the radiative fluxes. For thermal radiation, two components are considered: the downwelling thermal component (emitted from the atmosphere) and the upwelling thermal component (emitted from the surface). For solar radiation, the direct downwelling component from the sun, the diffuse downwelling component, and the surface-reflected solar radiation flux are considered. These five radiation components are computed from the solar and thermal data stored in ERA5; all procedures are detailed in Di Napoli et al. (2021b).

Finally, an operational procedure (Fiala et al. 2012) uses Ta, va, RH, and MRT to generate a UTCI-Fiala model gridded stack as output. The UTCI-Fiala model can predict the thermoregulatory reactions of the body system, considering vasoconstriction or vasodilation of skin blood flow, shivering thermogenesis, and sweat moisture excretion. The system was developed by a statistical regression (Fiala et al. 2001), using measured data from physiological experiments, covering steady-state and transient cold stress, cold, moderate, warm, and hot stress conditions, and activity levels of up to heavy exercise (Błażejczyk et al. 2010; Błażejczyk et al. 2013). Finally, the UTCI (°C) is derived from the UTCI-Fiala model, trying to represent the air temperature of a reference outdoor environment that would produce the same UTCI-Fiala modeled physiological response under actual environmental temperature conditions (Jendritzky et al. 2012).

2.2 Köppen–Geiger climatology

The Köppen–Geiger climatology was obtained from Beck et al. (2018), with 1-km -spatial resolution considering the 1980–2016 period, which is freely available at http://www.gloh2o.org/koppen/. The SA domain is characterized by seventeen climatic classes (Fig. 1), but we only considered the most representative, i.e., the classes with more than 2% of coverage area pixels. We thus obtained ten classes that

Fig. 1 Köppen–Geiger climate classification present-day map (1980–2016) for South America (Beck et al. 2018), highlighting the 31 cities with populations above 1 million (https://population.un.org/wup/Download/). Köppen–Geiger climate classes and relative area coverage of each class: Tropical Rainforest (Af –18%); Tropical Monsoon (Am – 15%); Tropical Savanna (Aw – 27%); Arid Desert Hot (BWh – 5%); Arid Desert Cold (BWk – 8%); Arid Steppe Hot (BSh – 1%); Arid Steppe Cold (BSk – 4%); Temperate, Hot-Dry Summer (CSa – <1%); Temperate Warm-Dry Summer (CSb – 1%); Temperate Dry-Winter, Hot Summer (Cwa – 2%); Temperate Dry-Winter, Warm Summer (Cwb – 1%); Temperate Dry-Winter, Cold Summer (Cwc – <1%); Temperate, no Dry season, Hot Summer (Cfa – 10%); Temperate, no Dry Season, Warm Summer (Cfb – 3%); Temperate, no Dry Season, Cold Summer (Cfc – <1%); Cold Dry-Warm Summer (Dsb – <1%); Cold Dry-Cold Summer (Dsc – <1%); Cold no Dry-Cold Summer (Dfc – <1%); Polar Tundra (ET – 4%)

encompass the Tropical Savanna (Aw); Tropical Rainforest (Af); Tropical Monsoon (Am); Temperate, no Dry season, Hot Summer (Cfa); Arid Desert Cold (BWk); Arid Steppe Hot (BSh); Polar Tundra (ET); Arid Steppe Cold (BSk); Temperate, no Dry Season, Warm Summer (Cfb); and Temperate Dry-Winter, Hot Summer (Cwa). To attribute a given UTCI pixel to a specific climate class, the Köppen–Geiger map was gridded at the same spatial resolution as the ERA5-HEAT grid.

In 2018, there were 371 cities with 1 million inhabitants or more worldwide, 46 of them located in SA. Regarding the world's 33 megacities (> 10 million inhabitants), 27 are in the South Hemisphere and 5 in SA, namely São Paulo, Rio de Janeiro, Buenos Aires, Lima, and Bogotá (United Nations-World Urbanization Prospects 2019).

For local analysis, a total of 31 SA cities with more than one million inhabitants (in 2018) were selected based on the United Nations report (United Nations 2022): (https://population.un.org/wup/Download/) (Table 1). Regarding the climatic zones, ten cities are in Aw class (Rio de Janeiro, Caracas, Fortaleza, Brasília, Guayaquil, Maracay, Assunción, Valencia, Santa Cruz de la Sierra, and Goiânia), six are Cfa (Buenos Aires, São Paulo, Porto Alegre, Montevideo, Rosario, Campinas), four are Cfb class (Bogotá, Cali, Curitiba, and Quito), other four are Af class (Salvador, Medellín, Manaus, and Belém), one is Am class (Recife), two are BSh (Maracaibo and Barranquilla), one is BWh (Lima), one is Cfc (Belo Horizonte), one is Cwa (Córdoba), and one is Csa (Santiago). For each city, the UTCI and Köppen–Geiger nearest pixel

Table 1 Köppen–Geiger (KG) climate classification for the thirty-one selected cities in South America, the respective population (in bold the most populated) from: https://population.un.org/wup/Download/

KG Class	City	Country	Pop 2018 (million)	Altitude(m)	Latitude (DMS)	Longitude (DMS)	UTCI annual (°C)	UTCI summer (°C)	UTCI winter (°C)
Af	Belém	Brazil	2.3	10	01°27′20″S	48°30′15″W	28.6	28.4	28.7
Af	Manaus	Brazil	2.1	92	03°07′01″S	60°01′34″W	29.6	29.3	29.2
Af	Medellin	Colombia	3.9	1,495	06°13′50″N	75°35′26″W	18.7	18.6	18.5
Af	Salvador	Brazil	3.7	8	12°58′28″S	38°28′36″W	24.4	26.0	22.1
Am	Recife	Brazil	4.0	10	08°04′03″S	34°55′00″W	26.3	28.0	24.0
Aw	Asuncion	Paraguay	3.2	43	25°18′23″S	57°39′28″W	21.5	28.4	14.8
Aw	Caracas	Venezuela	2.9	900	10°30′00″N	66° 54′59″W	25.5	23.8	26.2
Aw	Brasilia	Brazil	4.4	1,172	15°47′38″S	47°52′58″W	21.5	23.5	17.8
Aw	Fortaleza	Brazil	3.9	16	03°43′06″S	03°43′06″W	26.5	27.4	25.2
Aw	Goiania	Brazil	2.5	749	16°40′47″S	16°40′47W	23.4	25.1	19.8
Aw	Guayaquil	Ecuador	2.8	4	02°12′13″S	79°53′50″W	26.2	27.0	25.1
Aw	Maracay	Venezuela	1.2	445	10°14′48″N	67°36′23″W	25.2	24.0	25.4
Aw	Rio de Janeiro	Brazil	**13.2**	2	22°54′29″S	43°11′47″W	25.1	29.2	21.5
Aw	Santa Cruz de la Sierra	Bolivia	1.6	400	17°47′10″S	63°10′52″W	21.4	25.0	16.2
Aw	Valencia	Venezuela	1.9	520	10°09′23″N	67°59′58″W	25.0	23.8	25.4
Bsh	Barranquilla	Colombia	2.2	18	10°57′50″N	74°47′46″W	26.4	23.3	28.3
Bsh	Maracaibo	Venezuela	2.1	6	10°39′13″N	71°38′45″W	28.9	26.4	30.5
Bwh	Lima	Peru	**10.3**	3	12°02′46″S	77°02′34″W	20.6	23.9	17.6
Cfa	Campinas	Brazil	3.2	685	22°54′25″S	47°03′47″W	19.6	23.5	15.2
Cfa	Buenos Aires	Argentina	14.9	25	34°36′13″S	58°22′53″W	12.9	21.4	4.6
Cfa	Montevideo	Uruguay	1.7	43	34°54′04″S	56°09′52″W	13.1	21.0	5.2
Cfa	Porto Alegre	Brazil	4.1	10	30°01′59″S	51°13′48″W	18.6	24.9	12.4
Cfa	Rosario	Argentina	1.4	31	32°57′00″S	60°40′00″W	16.1	24.3	7.9
Cfa	São Paulo	Brazil	**24.6**	760	23°32′01″S	46°37′31″W	18.2	22.1	14.1
Cfb	Bogotá	Colombia	**10.5**	2,640	04°37′27″N	74°03′49″W	13.6	14.3	12.5
Cfb	Cali	Colombia	2.7	1,018	03°21′35″N	76°38′18″W	28.5	28.9	27.5
Cfb	Curitiba	Brazil	3.5	935	25°25′48″S	49°16′15″W	16.2	20.8	11.5
Cfb	Quito	Ecuador	1.8	2,850	00°10′50″S	78°28′04″W	15.0	14.9	15.0
Cfc	Belo Horizonte	Brazil	5.9	852	19°54′46″S	43°56′27″W	20.6	23.6	16.6
Csa	Santiago	Chile	6.6	570	33°26′50″S	70°40′25″W	10.6	17.4	3.3
Cwa	Cordoba	Argentina	1.5	389	31°25′00″S	64°11′00″W	16.0	24.1	7.5

Altitude (m), geographical coordinates in Degrees, Minutes, and Seconds (DMS), and UTCI (°C) average (annual, summer, and winter) for the 1979–2020 period

2.3 Heat classes and trends

Our analysis of SA is based on the study of Antonescu et al. (2021), who developed a bioclimatology of thermal stress for Europe in a 41 year-period (1979 − 2019) using UTCI derived from the ERA5-HEAT reanalysis and the Köppen–Geiger climate classification. Here, we used the same methodology, but for SA climate conditions, conducting a spatial–temporal analysis at the continental and local levels to evaluate the thermal stress from 1979 to 2020, using

the 1981–2010 climatology as reference period, as recommended by World Meteorological Organization (WMO 2017).

Considering air temperatures between -50 and 50 °C, Bröde et al. (2012) coupled the UTCI-Fiala model with the UTCI-clothing model and defined 10 universal human thermal stress categories, ranging from Extreme cold stress to Extreme heat stress based on UTCI values. Such categorization establishes the threshold for heat stress at a UTCI value of 26 °C. Since SA is located predominantly in the tropical and subtropical hot zones, we have performed a regional adjustment suggested by Krüger et al. (2021) based on the climatological UTCI values displayed in Table 1 and

determined the threshold for the thermal stress at 32 ℃. Moreover, this paper analyzes heat stress only. Thus, we considered two main categories for thermal stress, namely: i) -9 °C ≤ UTCI ≤ 32 °C (no thermal stress, NO STRESS); ii) UTCI > 32 °C (whole heat stress, HEAT). The HEAT category was also subdivided into two subcategories: iii) 32 °C ≤ UTCI ≤ 38 °C (strong heat stress, STRONG), and iv) UTCI > 38 °C (very strong/extreme heat stress, VSEXT).

For each grid cell in the SA domain and for each Köppen–Geiger class, we computed the fraction of hours from 1979 to 2020 within each of the three heat stress categories. Then, for each Köppen-Geiger class, we computed the UTCI trend value and analyzed the trends in the HEAT, STRONG, and VSEXT categories. We used the R language package Zhang + Yue-Pilon Trends (ZYP) (Bronaugh et al. 2023) to analyze the thermal stress trends using the nonparametric Mann–Kendall trend test (Kendall 1975) and considering 95% significance (p-value < 0.05). The package also whitened the data before trend estimation, using the procedure developed by Wang and Swail (2001).

For each of the thirty-three cities (Table 1), we conducted local-level analyses by computing the annual number of hours with heat stress anomalies in the HEAT, STRONG, and VSEXT categories. Finally, to analyze the changes in the number of consecutive hours with thermal stress we considered four-decade intervals (1980–1989, 1990–1999, 2000–2009, 2010–2019) for each city.

3 Results

3.1 Spatial distribution of heat stress from 1979–2020

Figure 2 shows the proportion of hours of NO STRESS, HEAT, STRONG, and VSEXT between 1979 and 2020 in SA. The largest number of hours with no-thermal stress conditions (> 86%) occurs over the western and southeastern coasts, especially around the Andes mountains. By contrast, fewer hours with no-thermal stress occur over the Amazon, and northern and central parts of SA (Fig. 2a). Most of the continent exhibits a large percentage of hours with heat stress (Fig. 2b) and strong heat stress (Fig. 2c), with a marked latitudinal northward increase. Hotspots for heat stress are located in the Equatorial zone (Fig. 2b), which presents 36% of the hours between 1979 and 2020 under heat stress. A large number of hours with strong heat stress (26–35%) occur over central-northern SA, especially around the Amazon region, and similar values are observed over parts of northeastern Brazil and Venezuela (Fig. 2c). Argentina, Paraguay, Uruguay, and the southeastern coast of Brazil show a low number of hours with strong heat stress (less than 15%). There is a clear inland/coastline contrast

in the number of hours under heat stress, in particular for very strong and extreme heat stress (Fig. 2d). For example, some central SA regions seem to be hotspots for very strong and extreme heat stress, such as central-western Brazil, Venezuela, and Paraguay. The north zone of the La Plata Basin, northeastern Brazil, and the Orinoco Basin present the highest percentage of very strong and extreme heat stress (5–10%) compared to other regions of the continent. Both western and eastern coastal zones are not affected by very strong and extreme heat stress.

3.2 Thermal stress trends in the Köppen-Geiger classes

The trends in the median annual number of hours with heat stress anomalies, relative to the 1981–2010 climatology, for the Köppen–Geiger classes were analyzed for HEAT, STRONG, and VSEXT classes as well as the trends of the median UTCI value (Fig. 3). In general, the annual number of hours within all categories of heat stress increased significantly between 1979 and 2020. For the HEAT category, all Köppen–Geiger classes show significant (p-value < 0.05) positive trends. The classes with trends above 1 h/year are Aw (+ 8.25 h/year); BSh (+ 7.13 h/year); Am (+ 6.80 h/year); Cwa (+ 6.58 h/year); Af (+ 6.08 h/year); BWh (+ 4.04 h/year); Cfa (+ 3.25 h/year), BSk (+ 1.66 h/year), and BWk (+ 1.16 h/year). For the STRONG events, the same patterns are observed, where values of significant positive trends (higher than 1 h/year), in descending order, are Cwa (+ 4.56 h/year); Aw (+ 3.60 h/year); Af (+ 3.22 h/year); BSh (+ 3.01 h/year); Am (+ 2.98 h/year); BWh (+ 2.46 h/year; and Cfa (+ 2.31 h/year). In VSEXT, trends are also positive, namely Aw (+ 4.51 h/year); Am (+ 4.41 h/year); Af (+ 2.83 h/year); BWh (+ 2.46 h/year); and Cwa (+ 2.13 h/year). Regarding UTCI values, all the Köppen–Geiger classes present statistically significant increasing trends, varying from 0.010 °C/year (BWk, BSk, and Cfb) to 0.024 °C/year (Aw).

It is worth noting that in SA the highest trends in the median annual number of hours with heat stress anomalies prevail over the most frequent Köppen–Geiger classes (see Fig. 1). This means that, during the past four decades, the largest increase in hours under heat stress occurs in climatic classes that encompass around 93% of the continent (for instance, Af (18%); Am (15%); Aw (27%); BWh (5%); BSh (1%); BWk (8%); BSk (4%); Cwa (2%); Cfa (10%); Cfb (3%)). This is equivalent to saying that most of the SA continent exhibits an increase between 85 to 348 h of heat stress conditions, 85 to 183 h of strong heat conditions, and between 59 and 420 h under very strong and extreme heat conditions during the 1979–2020 period when compared to the baseline 1981–2010 climatology. Regarding the increasing trends observed in UTCI values, this is equivalent to
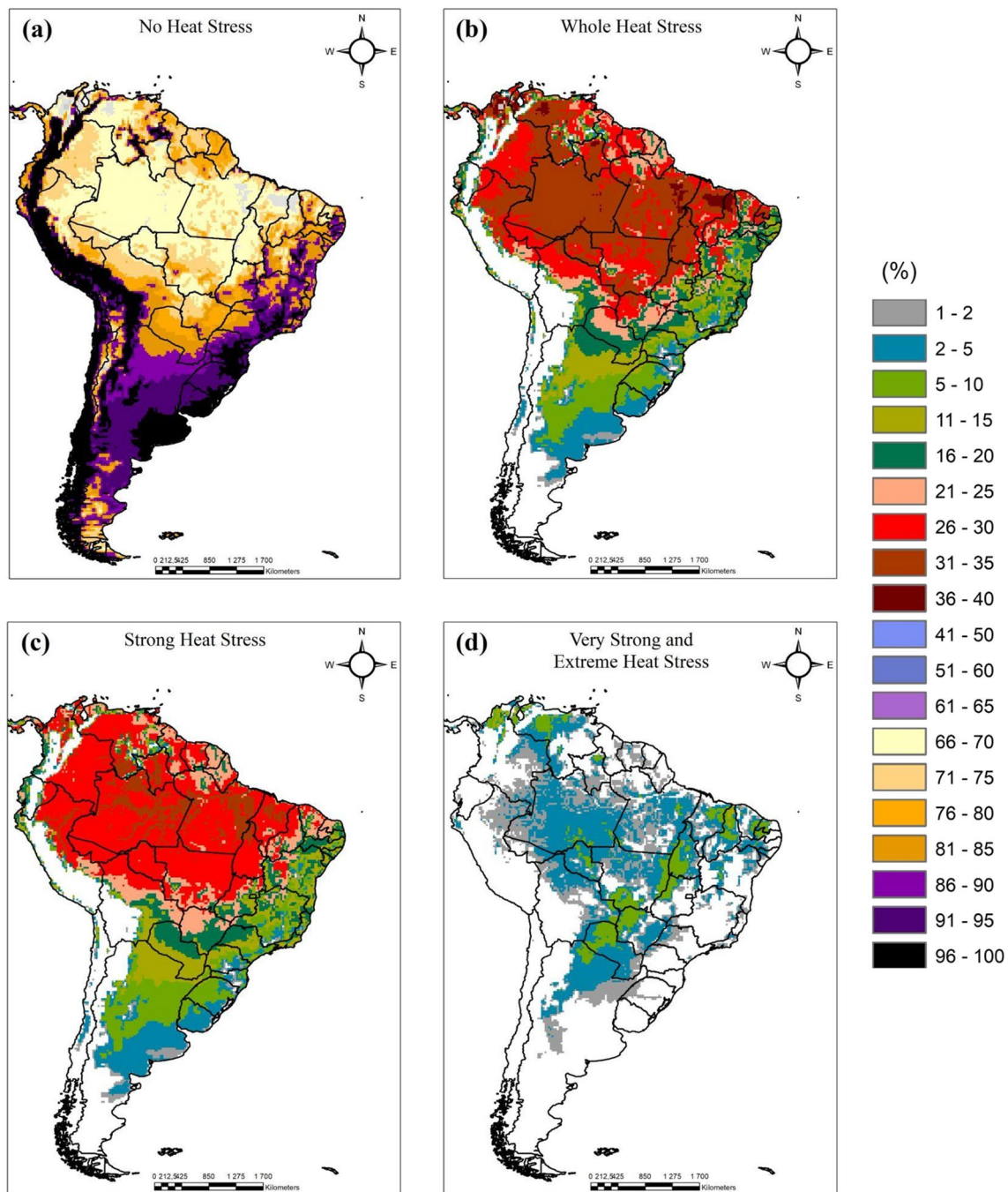
Fig. 2 Percentage of hours between 1979 and 2020 with (**a**) no heat stress (-13 ℃ ≤ UTCI ≤ 32 ℃), (**b**) whole heat stress (HEAT: UTCI > 32 ℃), (**c**) strong heat stress (STRONG: 32 ℃ ≤ UTCI ≤ 38 ℃) and (**d**) very strong and extreme heat classes (VSEXT: UTCI > 38 ℃), from the total number of hours in each grid cell. Percentages below 0.1% are in white

an increase ranging from 0.41 to 0.98 °C during the study period.

3.3 Thermal stress trends for South American Cities

The annual number of hours with HEAT, STRONG, and VSEXT stress anomalies relative to the 1981–2010 period for the 31 South American cities are shown in Figs. 5, 6 and 7, respectively. Those results highlight that the past 20 years (from 2000 forward) presented more hours of heat stress than the previous two decades in all the cities in SA in all heat stress categories.

For the HEAT stress category (Fig. 4), among the 31 cities, only five showed no trends, namely Bogotá, Cali,

Fig. 3 Median annual number of hours with HEAT (first column), STRONG (second column) and VSEXT (third column), and UTCI (fourth column) stress anomalies (relative to 1981–2010) for the ten main Köppen–Geiger classes in SA between 1979 and 2020. Statistically significant trends (hours per year) for each class are marked with a rectangle (p < 0.05 using the Mann–Kendall trend test)

Medellín, Quito, and Montevideo; and eight cities showed non-significant trends, namely Guayaquil, Recife, Santiago, Salvador, Caracas, Porto Alegre, Lima, and Barranquilla. The remaining 18 cities showed significant positive trends (from highest to lowest): Maracaibo (13.59 h/year), Fortaleza (13.13 h/year), Goiania (12.98 h/year), Brasilia (10.13 h/year), Maracay (9.81 h/year), Santa Cruz de la Sierra (9.46 h/year), Campinas (9.39 h/year), Manaus (8.31 h/year), Belo Horizonte (7.87 h/year), Valencia (6.71 h/year), Asuncion (6.41 h/year), Rio de Janeiro (6.37 h/year), São Paulo (6 h/year), Cordoba (4.53 h/year), Belem (4.10 h/year), Rosario (3.59 h/year), Buenos Aires (2.47 h/year), and Curitiba (1.79 h/year).

Regarding the STRONG stress category (Fig. 5), in addition to the five previous cities (Bogotá, Cali, Medellín,

Quito, and Montevideo), Manaus and Porto Alegre presented no trends (less than 1 h/year). In contrast to the HEAT stress category, the city of Barranquilla showed a significant trend for STRONG heat stress. However, in the cities of Rio de Janeiro and Asuncion, although positive trends were greater than 1 they were not significant. A total of eight cities presented no significant trends, namely Guayaquil, Recife, Santiago, Salvador, Caracas, Porto Alegre, Lima, and Rio de Janeiro. Significant positive trends were observed in 16 cities (from highest to lowest): Fortaleza (13.5 h/year), Goiania (11.45 h/year), Maracay (10.35 h/year), Brasília (9.95 h/year), Campinas (9.05 h/year), Santa Cruz de la Sierra (8.55 h/year), Belo Horizonte (7.7 h/year), Valencia (7.4 h/year), São Paulo (6.03 h/year), Barranquilla (5.05 h/year), Maracaibo (4.65 h/year), Belém (3.85 h/year), Cordoba
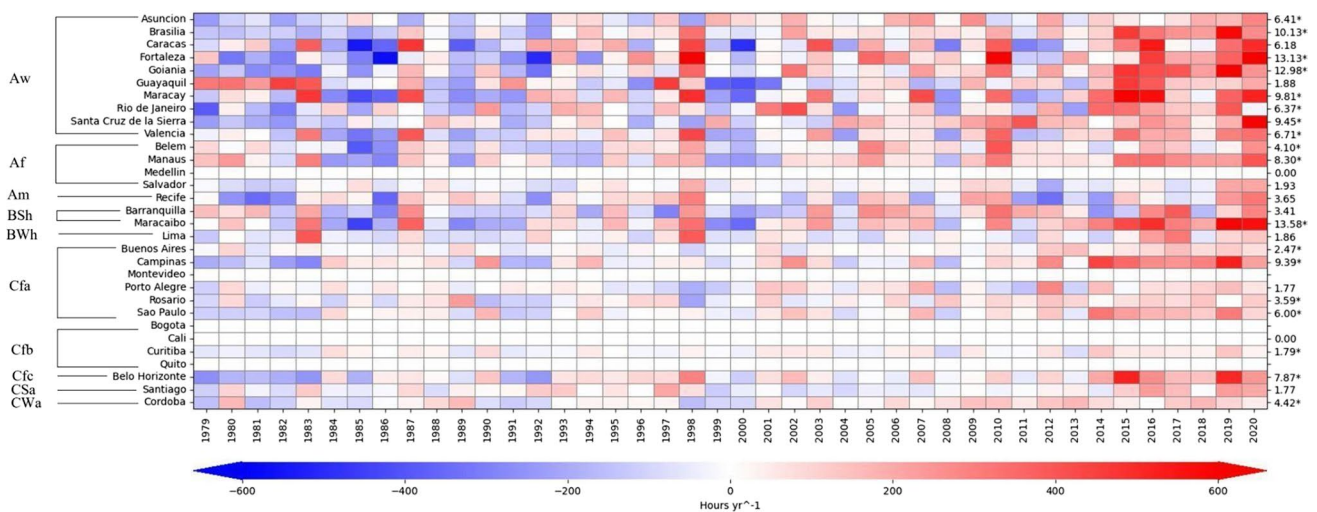
Fig. 4 Number of hours/year with HEAT stress anomalies (hours, relative to 1981–2010, shaded according to the scale) for 31 South American cities. The Köppen-Geiger subclass for each city is indicated on the left. The trend (hr year-1) calculated using the Theil-Sen slope estimator for each city is shown on the right. Statistical significance at $p < 0.05$ using the Mann–Kendall trend test is indicated with an asterisk
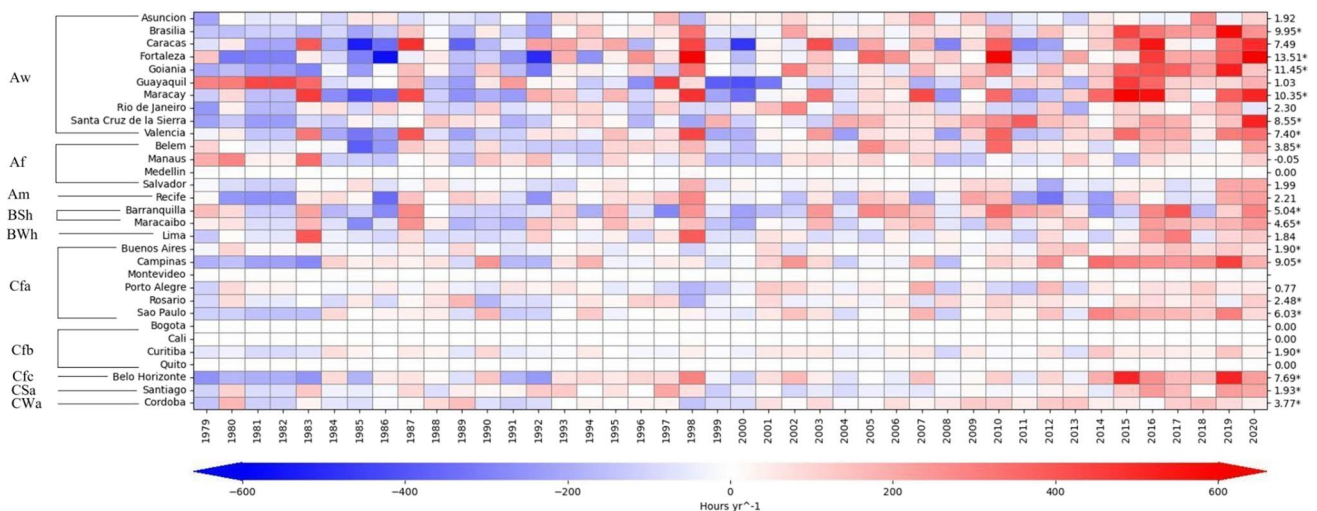

Fig. 5 Same as Fig. 5 but for the STRONG heat caetgory

(3.78 h/year), Rosario (2.5 h/year), Buenos Aires (1.9 h/year), and Curitiba (1.9 h/year).

In VSEXT (Fig. 6), 26 cities showed no trends. Five cities showed positive and significant trends: Manaus (8.11 h/year), Maracaibo (7.4 h/year), Asuncion (4.63 h/year), Rio de Janeiro (4.1 h/year), and Goiania (1.12 h/year). Despite not showing significant or considerable trends in the STRONG category, Rio de Janeiro, Asuncion, and Manaus have high and significant trends in VSEXT, which are close to the whole HEAT category trends. Thus, the behavior of those cities in the VSEXT category modulates the observable trends in the HEAT category.

3.4 Changes in the number of consecutive hours with thermal stress for SA cities

For the analysis of the number of consecutive hours with thermal stress, ten cities were selected based on higher significant heat stress trends within different Köppen–Geiger sub-classes. The cities are Asuncion (Aw), Buenos Aires (Cfa), Brasilia (Aw), Cordoba (Cwa), Fortaleza (Aw), Manaus (Af), Maracaibo (BSh), Rio de Janeiro (Aw), São Paulo (Cfa), and Santa Cruz de la Sierra (Aw). Figures 7, 8, and 9 show the number of consecutive hours in HEAT, STRONG, and VSEXT, respectively, considering a 10-year
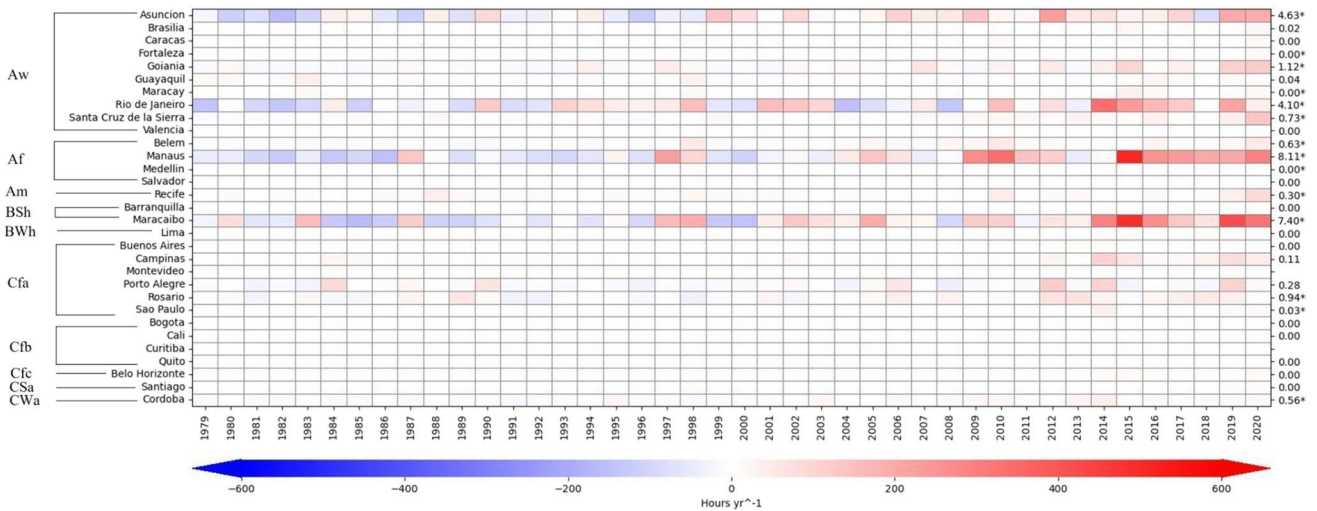
Fig. 6 Same as Fig. 5 but for the VSEXT heat stress category
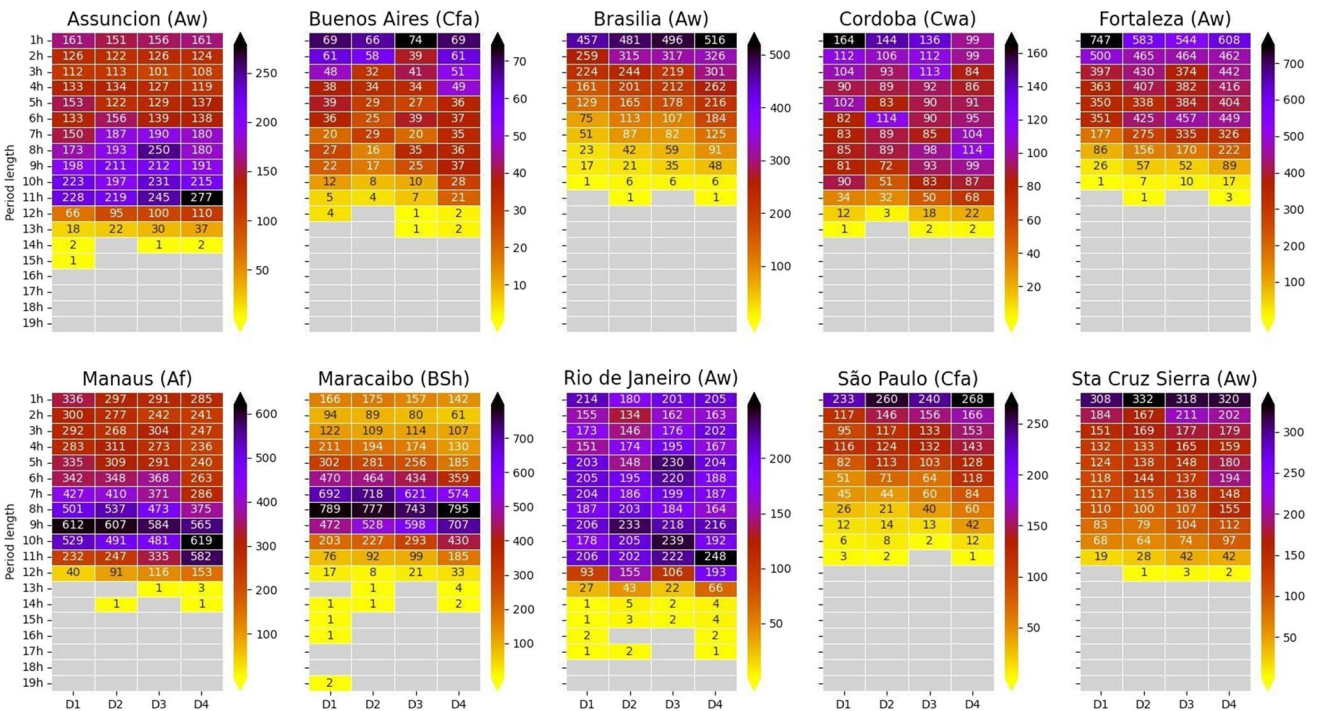

Fig. 7 Number of cases with consecutive hours under HEAT stress (period of length from 1 and 19 consecutive hours) for Asuncion, Buenos Aires, Brasilia, Cordoba, Fortaleza, Manaus, Maracaibo, Rio de Janeiro, São Paulo, and Sta. Cruz de la Sierra, for periods 1980–1989 (D1), 1990–1999 (D2), 2000–2009 (D3), and 2010–2019 (D4). Null cases are in gray

interval encompassing 4 different decades: 1980–1989 (D1), 1990–1999 (D2), 2000–2009 (D3), and 2010–2019 (D4). The aim of this analysis was to evaluate changes in the number of cases with consecutive hours (period length between 1 and 19 h) under heat stress over the past four decades.

For the HEAT category, four cities presented an increase in the number of consecutive hours under heat stress

conditions. The largest number of cases with consecutive hours with heat stress for Asuncion (Aw) during decade D1 (1980–1989) was found in the period length of 7–9 consecutive hours (27.8%) while for decade D4 (2010–2019), it shifted to the maximum of 10–12 consecutive hours (31.3%). The same applies to Cordoba (Cwa), Manaus (Af), and Rio de Janeiro (Aw), where these shifts were from
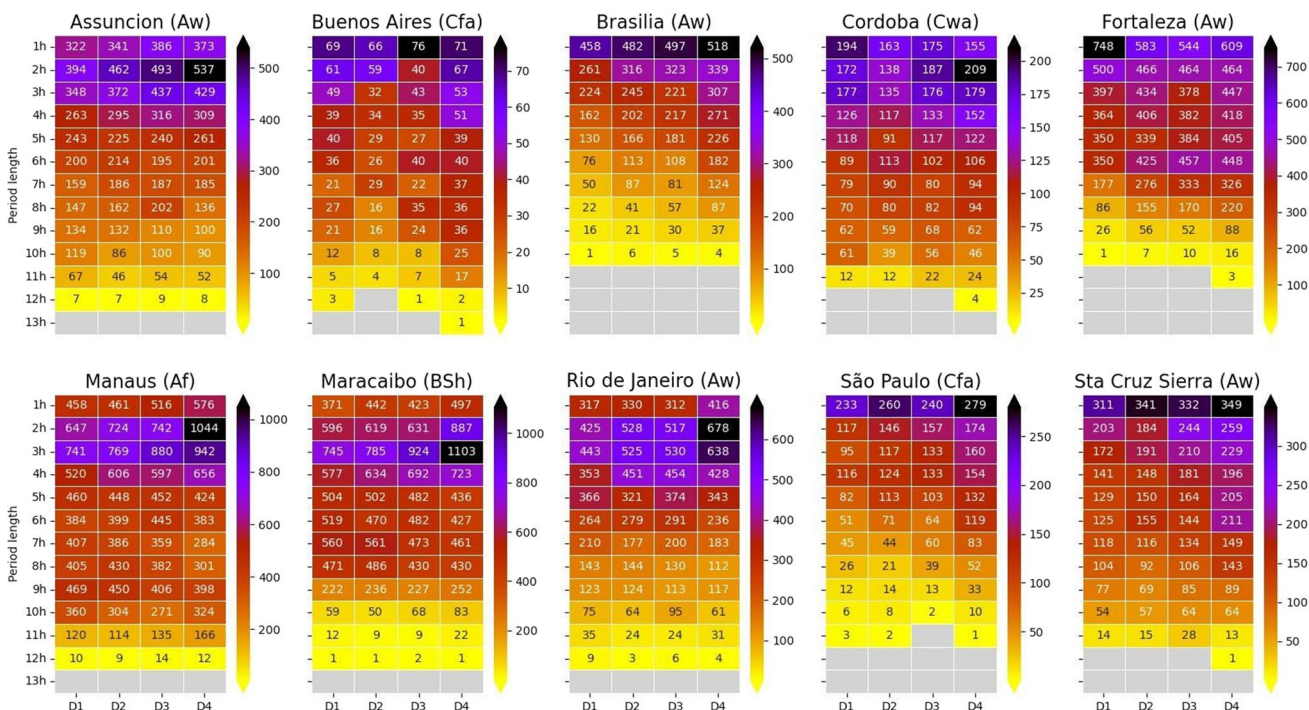
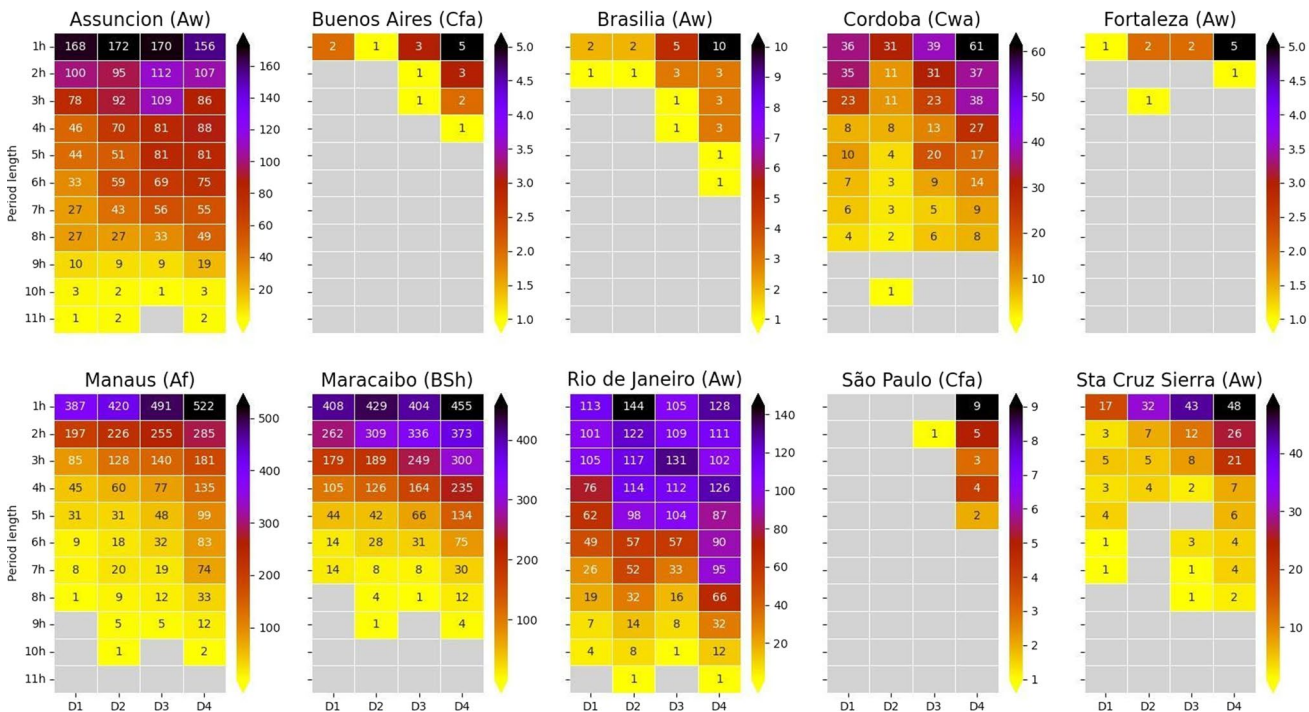**Fig. 8** Same as Fig. 8 but for the STRONG heat category

Fig. 9 Same as Fig. 8 but for the VSEXT heat category

1–3 h (36.5%), 7–9 h (36.4%), and 7–9 h (27.0%) in D1 to 7–9 h (32.9%), 10–12 h (32.2%) and 10–12 h (28.6%) in D4, respectively. These shifts reflect an increase in the

persistence of consecutive hours under heat stress over the past four decades. The remaining cities present a clear increase in length from D1 to D4. For instance, in Buenos

Aires (Cfa) the number of cases with 7–9 (10–12) consecutive hours of heat stress grew from 18.1% (5.5%) in D1 to 33.9% (16.0%) in D4. In Brasilia (Aw), São Paulo (Cfa), and Fortaleza (Aw) these changes were from 6.5%, 10.5%, and 9.6% (D1) to 15.7%, 20.2%, and 20.3% (D4) in the case of 7–9 consecutive hours, respectively. In Maracaibo (Bsh) and Santa Cruz de la Sierra (Aw), we found a shift from 8.2% and 6.1% (D1) to 17.7% and 9.6% (D2) in the case of 10–12 consecutive hours, respectively.

For the STRONG category, all cities exhibited an increase in the number of consecutive hours under strong heat stress over the last four decades. For example, for 2 (7) consecutive hours under strong heat stress, this value was 36% (133%) higher in D4 than in D1 in Asuncion (Aw) (São Paulo (Cfa)). The number of cases for 8–11 consecutive hours in Buenos Aires (Cfa) and Fortaleza (Aw) increased from D1 to D4, from 76 to 240%, and from 155 and 1500%, respectively. In Brasilia (Aw) for 8 to 10 consecutive hours, this increase ranged from 295 to 300%. The cases under VSEXT are similarly more frequent in D4 than in D1 for all regions and period lengths. For instance, the number of cases with 6 consecutive hours in this category in D1 almost doubled that of D4 in Cordoba (Cwa), Rio de Janeiro (Aw), and Asuncion (Aw), and was 9 and 5 times higher in Manaus (Af) and Maracaibo (BSh), respectively. It is worth noting that in São Paulo (Cfa) consecutive hours under VSEXT stress were only detected during 2010–2019 (D4).

4 Discussion

South America's large latitudinal (from 10°N to 55°S) and orographic (mountains, highlands, river basins, and coastal plains) variations contribute to the observed geographical north–south and west–east differences in observed heat stress. The contribution of topography and latitude to UTCI variability was previously reported for different regions of the globe such as China (Zeng et al. 2020; Ge et al. 2017), Russia (Vinogradova 2021), and Europe (Antonescu et al. 2021; Di Napoli et al. 2018). For instance, the distribution of the NO HEAT stress category observed in the present study over the higher latitudes of SA is consistent with results obtained for the northern hemisphere in those studies. The Equator-to-pole thermal gradient, which dominates low-level air temperatures over the continent (Garreaud et al. 2009), also triggers heat stress that prevails over the tropical belt, in line with the high influence of solar radiation on UTCI (Pappenberger et al. 2015). The global climatology of the UTCI by Di Napoli et al. (2021b) highlighted the equatorial regions with a prevalence of heat stress category, which agrees with our results. Since UTCI-HEAT is derived from the UTCI-Fiala model (Fiala et al. 2012), temperature and relative humidity are

the main drivers in the internal heat exchange mechanism. Studies conducted in China (Ge et al. 2017) showed that the UTCI decreases with increasing altitude (due to lower temperatures and humidity), which corroborates our results of no heat stress prevalence over the Andes mountains. The Andes, the longest world and highest (outside Asia) mountain range (8,900 km in length, 200–700 km wide, and 4,000 km in height) extending from north to south direction along the western edge of SA through Venezuela, Colombia, Ecuador, Peru, Bolivia, Chile, and Argentina, also plays a critical role in the distinct temperature and humidity patterns between the western and eastern SA coasts (Garreaud et al. 2009). This partially explains the heat stress difference between the Pacific and Atlantic coastal zones as reported here. Other factors can also play an important role in the east–west and inland-coastline asymmetries of heat stress, such as the continental asymmetry (wide at low latitudes and narrow at midlatitudes) and the different boundary patterns imposed by the Pacific and Atlantic oceans. By contrast to the warm southwestern Atlantic, the southeastern Pacific presents a predominance of the upwelling of cold waters, which induces a great cooling influence in the western SA coast by the sea breeze (Belmadani et al. 2014). Accordingly, also forced by the presence of the Andes, there are dry and cooler conditions prevailing along the Pacific coastline, while warm and humid conditions are predominant over the Atlantic coast through the inland of the continent to the Andes. Strong and extreme heat stress occurs in specific regions such as the north zone of the La Plata Basin, northeastern Brazil, and the Orinoco Basin. These regions are recognized as hotspots of strong land–atmosphere interactions in the continent which contribute to soil moisture anomalies and consequently to the intensification and persistence of high-temperature episodes (Menéndez et al. 2019; Spennemann et al. 2018).

The rising UTCI trend and consequently heat stress over the past four decades observed here in all Köppen–Geiger classes of SA correlate well with the current changes in the temperature and precipitation patterns observed in the region. Mean temperatures over SA have increased by ~ 0.15 °C per decade from 1961 to 2015, with distinct rates around the continent (IPCC interactive atlas, Gutiérrez et al. 2021, Iturbide et al. 2021). There is clear evidence that an increase in HW intensity, frequency, and duration is widespread in SA, specifically, from 1995 onwards, with a huge enhancement since 2000 (Ceccherini et al. 2016). The frequency of HWs during austral summer has doubled in northern SA, while smaller increases have been noted in the southern (Feron et al. 2019). A decrease in the frequency of cold extremes and an increase in the occurrence of warm extremes was observable in many regions of the continent (Rusticucci et al. 2016; Regoto et al. 2021).

In addition, prolonged periods of extremely hot temperatures are increasingly connected with dry periods over the past two decades, and the continent is seeing two thirds of its area under increased susceptibility to these compound events (Mukherjee et al. 2022). Northeastern and southeastern SA and the Amazon basin were some of the zones with a rise in the frequency, duration, and magnitude of compound drought and HW events per year since 2000 (Feng et al. 2020; Libonati et al. 2022b). The above-mentioned zones coincide with those Köppen–Geiger climatic zones presenting, in this study, the highest trends in the median annual number of hours with heat stress (strong, very strong, and extreme) anomalies, which reinforces our findings. The reason behind the different UTCI trend rates in the different Köppen–Geiger classes may be attributed to regional patterns associated with the complex interplay and feedback between climate and land cover changes (Cui et al. 2021). Nevertheless, the persistence of hours under heat stress implies undoubtedly the fact that the population is being progressively exposed to unhealthy heat conditions. Through the twenty-first century, up to 20% of the continental area is expected to undergo changes in the Köppen–Geiger climate zone under the high-emission scenario, especially, arid and hot climates in the tropics and subtropics are projected to face a poleward expansion (Chan and Wu 2015). In this context, the expected continuous warming of SA (Meng et al. 2022) will impact the well-being of at least 2 to 6 million people in southeastern SA, 1–4 million people over the west coast of SA, 1–5 million people in the Amazon basin and around 1–5 million people in northeastern SA (Liu et al. 2021).

The twenty-first century is the first "urban century", according to the United Nations Development Programme, since the majority of the world's population (57% by 2020) is living in urban areas (United Nations-World Urbanization Prospects 2019). The SA population underwent its main urbanization process in the late 1970s when urban residents accounted for 60% of the total population. In 1990, this proportion exceeded 75% of the continent's population and reached 85% in 2020 (United Nations-World Urbanization Prospects 2019). Pervasive spatial growth has been noticed in main SA cities over the last decades at faster rates when compared to other regions in the world (Inostroza et al. 2013). Urban expansion has resulted in changes in the environment and in the local climate, including the urban heat island effect (UHI) (He et al. 2021). The alteration of the local climate can be described by warmer temperatures, lower humidity, and ventilation, higher atmospheric pollution, poor environmental quality, or more complex indicators of bioclimatic comfort (Qabbal et al. 2022). In particular, the UHI effect has great potential to amplify warm conditions within urban areas (Peres et al. 2018; Miranda et al. 2022) and consequently heat stress (Di Napoli et al. 2021b).

Superimposed on the ongoing global warming trend, SA's 21st-century urbanization (both in terms of the built-up area and the number of urban inhabitants (United Nations-World Urbanization Prospects 2019) explains the progressive rise in the number of hours/year with heat and strong heat stress anomalies over the last 4 decades, in particular over the last two decades. These results are in line with the observed increase in UHI intensities in SA, which has warmed by 0.05 K/year since 2003 (Mentaschi et al. 2022). By contrast to inland regions, the sea breeze cooling effect in coastal cities attenuates the UHI, as previously observed in Buenos Aires and São Paulo, but this effect can be inhibited by buildings acting like barriers for breeze around the city (Freitas et al. 2007). Besides, UHI can also contribute to exacerbating the effect of HW in urban areas (Henríquez and Romero 2019). Positive trends in the number of HWs in Brazilian cities (e.g. Manaus, Recife, Brasilia, Rio de Janeiro, São Paulo, and Porto Alegre) were linked to the urbanization effect (Geirinhas et al. 2018).

It is worth mentioning that results show that Manaus, a 2 million population city located in the center of the Amazon rainforest, presented the highest trends in the number of hours under very strong and extreme heat stress. Those results are in line with recent studies which indicate that this region has undergone intense urbanization in the past four decades (de Souza et al. 2016). In addition, this region has been facing the highest increasing frequency in the number of hot days since 1961 among other regions in Brazil (Regoto et al. 2021) as well as in the number of HW events (Geirinhas et al. 2018), thus corroborating our results. Also, three other cities have been highlighted by the very strong and extreme heat class: Maracaibo, Asuncion, and Rio de Janeiro. Maracaibo has a hot-humid climate type (González Cruz and Krüger 2015), similar to the Amazonian. Asuncion has recently faced, together with the whole of central south-America, an intense heat wave in 2020, where maximum temperatures reached 43.1 °C (Marengo et al. 2022). In Rio de Janeiro, recent studies (Geirinhas et al. 2021, 2022) have shown a substantial contribution of persistent dry conditions to severe heatwave episodes, and substantial increases have been observed in the occurrence of these compound events. Another city that has increased the number of hours of heat stress was Buenos Aires, which has also registered numerous heat waves during the twentieth century and the beginning of the twenty-first century (Chesini et al. 2019). In the past decade, from the warm semester 2004/2005 to 2013/2014, there has been at least one episode of HW per year.

The ERA5-HEAT dataset is a valuable tool to analyze heat stress and has been used in a lot of worldwide works, mostly because it uses wind and radiation information, which is usually underrated in many heat stress models (Di Napoli et al. 2021a). Hence our study is one of few works on UTCI for SA, and the first one to analyze the ERA5-HEAT

at a continental scale. However, systematic errors are common amongst current reanalyses and are mostly related to resolution issues. Thus, it is important to work on the further development of better local calibrations, as suggested by Silva and Hirashima ([2021](#)). A comparison between different indices should also be encouraged as different heat stress levels vary depending on how temperature and humidity are considered in the equations (Freychet et al. [2022](#)). In addition, reanalyses like ERA5 have inhomogeneities related to resolution as well as to data assimilation, where intercomparison and evaluation studies with different reanalysis outputs, forcing UTCI, should be considered.

5 Conclusions

Here we present the first comprehensive bioclimatology of thermal stress in SA over the past four decades based on the spatial and temporal variations of UTCI. The hotspots of higher frequency of hours under heat stress occurred in the central-northern SA, and northeastern Brazil, reflecting a huge east–west and inland-coastline contrast. These patterns highlight the influence of South American topography, geographical asymmetry, as well as the different thermal characteristics of the Pacific and Atlantic oceans. South America's extensive latitudinal range also impacts heat stress patterns. Moving northward, heat stress hours increase due to the equator-to-pole thermal gradient, resulting in higher temperatures and more heat stress in the tropical and subtropical regions. Results revealed that prolonged periods of heat stress increased significantly between 1979 and 2020, but particularly since the 2000', for all major populated cities and in all heat stress categories. Overall, there has been an increase not only in the number of consecutive hours under heat stress but also in the persistence of such extremes within Köppen–Geiger climatic classes which encompass 93% of the continent.

Worldwide, extremely hot conditions are becoming more frequent, intense, and long-lasting and these trends are projected to be exacerbated in the future due to climate change (Perkins-Kirkpatrick and Lewis [2020](#)). The World Health Organization recognizes global warming as the main global health threat of the 21st Century, highlighting regions with the poorest health infrastructure as hotspots of high vulnerability. However, the global distribution of knowledge regarding heat stress is mainly clustered in higher-income regions of the North Hemisphere and Australia, with tropical and subtropical regions of the South Hemisphere being underrepresented (Campbell et al. [2018](#)). Accordingly, we argue that response capacity to population exposure in lower-income regions, such as SA, requires robust and updated knowledge about the spatial–temporal distribution of heat stress, as provided in this study. Furthermore, the results presented here can be associated with socio-economic data, including population density, average income, public health infrastructure, land use changes, education level, and other factors, aiming to determine tools and frameworks for risk assessment and mitigation strategies, which certainly motivates future works.

Declarations

References

Ahima RS (2020) Global warming threatens human thermoregulation and survival. J Clin Investig 130:559–561. https://doi.org/10.1172/JCI135006

Antonescu B, Mărmureanu L, Vasilescu J, Marin C, Andrei S, Boldeanu M, Ene D, Ţilea A (2021) A 41-year bioclimatology of thermal stress in Europe. Int J Climatol 41:3934–3952

Barreca A, Schaller J (2020) The impact of high ambient temperatures on delivery timing and gestational lengths. Nat Clim Chang 10:77–82. https://doi.org/10.1038/s41558-019-0632-4

Beck HE, Zimmermann NE, McVicar TR, Vergopolan N, Berg A, Wood EF (2018) Present and future Köppen-Geiger climate classification maps at 1-km resolution. Sci Data 5:180214. https://doi.org/10.1038/sdata.2018.214

Belmadani A, Echevin V, Codron F, Takahashi K, Junquas C (2014) What dynamics drive future wind scenarios for coastal upwelling off Peru and Chile? Clim Dyn 43:1893–1914. https://doi.org/10.1007/s00382-013-2015-2

Błażejczyk K, Broede P, Fiala D, Havenith G, Holmér I, Jendritzky G, Kampmann B, Kunert A (2010) Principles of the New Universal Thermal Climate Index (UTCI) and its Application to Bioclimatic Research in European Scale. Miscellanea Geograph 14:91–102. https://doi.org/10.2478/mgrsd-2010-0009

Błażejczyk K, Jendritzky G, Bröde P, Fiala D, Havenith G, Epstein Y, Psikuta A, Kampmann B (2013) An introduction to the Universal Thermal Climate Index (UTCI). Geogr Pol 86:5–10. https://doi.org/10.7163/GPol.2013.1

Bröde P, Fiala D, Błażejczyk K, Holmér I, Jendritzky G, Kampmann B, Tinz B, Havenith G (2012) Deriving the operational procedure for the Universal Thermal Climate Index (UTCI). Int J Biometeorol 56:481–494. https://doi.org/10.1007/s00484-011-0454-1

Bröde P, Blazejczyk K, Fiala D, Havenith G, Holmér I, Jendritzky G, Kuklane K, Kampmann B (2013) The Universal Thermal Climate Index UTCI compared to ergonomics standards for assessing the thermal environment. Ind Health 51:16–24. https://doi.org/10.2486/indhealth.2012-0098

Bronaugh D, Werner A, Bronaugh MD (2023) Package 'zyp.' CRAN Repository. https://cran.r-project.org/. Accessed Sept 2023

Campbell S, Remenyi TA, White CJ, Johnston FH (2018) Heatwave and health impact research: A global review. Health Place 53:210–218. https://doi.org/10.1016/j.healthplace.2018.08.017

Ceccherini G, Russo S, Ameztoy I, Romero CP, Carmona-Moreno C (2016) Magnitude and frequency of heat and cold waves in recent decades: the case of South America. Nat Hazards Earth Syst Sci 16(3):821-831

Chan D, Wu Q (2015) Significant anthropogenic-induced changes of climate classes since 1950. Sci Rep 5:13487. https://doi.org/10.1038/srep13487

Cheng J, Bambrick H, Yakob L, Devine G, Frentiu FD, Toan DTT, Thai PQ, Xu Z, Hu W (2020) Heatwaves and dengue outbreaks in Hanoi, Vietnam: New evidence on early warning. PLoS Negl Trop Dis 14:e0007997. https://doi.org/10.1371/journal.pntd.0007997

Cheshire WP (2016) Thermoregulatory disorders and illness related to heat and cold stress. Auton Neurosci 196:91–104. https://doi.org/10.1016/j.autneu.2016.01.001

Chesini F, Abrutzky R, Titto ED (2019) Mortalidad por olas de calor en la ciudad de Buenos Aires, Argentina (2005–2015). Cad. Saúde Pública 35:e00165218. https://doi.org/10.1590/0102-311x00165218

Costa DF, Gomes HB, Silva MCL, Zhou L (2022) The most extreme heat waves in Amazonia happened under extreme dryness. Clim Dyn 59:281–295. https://doi.org/10.1007/s00382-021-06134-8

Cramer MN, Jay O (2016) Biophysical aspects of human thermoregulation during heat stress. Auton Neurosci 196:3–13. https://doi.org/10.1016/j.autneu.2016.03.001

Cui D, Liang S, Wang D (2021) Observed and projected changes in global climate zones based on Köppen climate classification. WIREs Clim Chang 12. https://doi.org/10.1002/wcc.701

Di Napoli C, Messeri A, Novák M, Rio J, Wieczorek J, Morabito M, ..., Pappenberger F (2021a) The Universal Thermal Climate Index as an operational forecasting tool of human biometeorological conditions in Europe. Applications of the Universal Thermal Climate Index UTCI in Biometeorology: Latest Developments and Case Studies, 193–208

Di Napoli C, Barnard C, Prudhomme C, Cloke HL, Pappenberger F (2021b) ERA5-HEAT: a global gridded historical dataset of human thermal comfort indices from climate reanalysis. Geosci Data J 8(1):2-10

Di Napoli C, Pappenberger F, Cloke HL (2018) Assessing heat-related health risk in Europe via the Universal Thermal Climate Index (UTCI). Int J Biometeorol 62:1155–1165. https://doi.org/10.1007/s00484-018-1518-2

Di Napoli C, Pappenberger F, Cloke HL (2019) Verification of heat stress thresholds for a health-based heat-wave definition. J Appl Meteorol Climatol 58:1177–1194. https://doi.org/10.1175/JAMC-D-18-0246.1

Feng S, Wu X, Hao Z, Hao Y, Zhang X, Hao F (2020) A database for characteristics and variations of global compound dry and hot events. Weather Clim Extremes 30:100299. https://doi.org/10.1016/j.wace.2020.100299

Feron S, Cordero RR, Damiani A, Llanillo PJ, Jorquera J, Sepulveda E, Asencio V, Laroze D, Labbe F, Carrasco J, Torres G (2019) Observations and projections of heat waves in South America. Sci Rep 9:8173. https://doi.org/10.1038/s41598-019-44614-4

Fiala D, Lomas KJ, Stohrer M (2001) Computer prediction of human thermoregulatory and temperature responses to a wide range of environmental conditions. Int J Biometeorol 45:143–159. https://doi.org/10.1007/s004840100099

Fiala D, Havenith G, Bröde P, Kampmann B, Jendritzky G (2012) UTCI-Fiala multi-node model of human heat transfer and temperature regulation. Int J Biometeorol 56:429–441. https://doi.org/10.1007/s00484-011-0424-7

Florido Ngu F, Kelman I, Chambers J, Ayeb-Karlsson S (2021) Correlating heatwaves and relative humidity with suicide (fatal intentional self-harm). Sci Rep 11:22175. https://doi.org/10.1038/s41598-021-01448-3

Freitas ED, Rozoff CM, Cotton WR, Dias PLS (2007) Interactions of an urban heat island and sea-breeze circulations during winter over the metropolitan area of São Paulo, Brazil. Boundary-Layer Meteorol 122:43–65. https://doi.org/10.1007/s10546-006-9091-3

Freychet N, Hegerl GC, Lord NS, Lo YTE, Mitchell D, Collins M (2022) Robust increase in population exposure to heat stress with increasing global warming. Environ Res Lett 17:064049. https://doi.org/10.1088/1748-9326/ac71b9

García-Witulski CM, Rabassa MJ (2021) The impact of temperature on mortality in Argentinean Municipalities. In The Economics of Climate Change in Argentina (pp. 3-15). Cham: Springer International Publishing

Garreaud RD, Vuille M, Compagnucci R, Marengo J (2009) Present-day South American climate. Palaeogeogr Palaeoclimatol Palaeoecol 281:180–195. https://doi.org/10.1016/j.palaeo.2007.10.032

Ge Q, Kong Q, Xi J, Zheng J (2017) Application of UTCI in China from tourism perspective. Theor Appl Climatol 128:551–561. https://doi.org/10.1007/s00704-016-1731-z

Geirinhas JL, Trigo RM, Libonati R, Coelho CAS, Palmeira AC (2018) Climatic and synoptic characterization of heat waves in Brazil. Int J Climatol 38:1760–1776. https://doi.org/10.1002/joc.5294

Geirinhas JL, Trigo RM, Libonati R, Castro LCO, Sousa PM, Coelho CAS, Peres LF, Magalhães MDAFM (2019) Characterizing the atmospheric conditions during the 2010 heatwave in Rio de Janeiro marked by excessive mortality rates. Sci Total Environ 650:796–808. https://doi.org/10.1016/j.scitotenv.2018.09.060

Geirinhas JL, Russo A, Libonati R, Sousa PM, Miralles DG, Trigo RM (2021) Recent increasing frequency of compound summer drought and heatwaves in Southeast Brazil. Environ Res Lett 16:034036. https://doi.org/10.1088/1748-9326/abe0eb

Geirinhas JL, Russo AC, Libonati R, Miralles DG, Sousa PM, Wouters H, Trigo RM (2022) The influence of soil dry-out on the record-breaking hot 2013/2014 summer in Southeast Brazil. Sci Rep 12:5836. https://doi.org/10.1038/s41598-022-09515-z

González Cruz E, Krüger E (2015) Evaluating the potential of an indirect evaporative passive cooling system for Brazilian dwellings. Build Environ 87:265–273. https://doi.org/10.1016/j.buildenv.2015.01.020

Guo Y, Gasparrini A, Armstrong BG, Tawatsupa B, Tobias A, Lavigne E, Coelho MDSZS, Pan X, Kim H, Hashizume M, Honda Y, Guo Y-LL, Wu C-F, Zanobetti A, Schwartz JD, Bell ML, Scortichini M, Michelozzi P, Punnasiri K, Li S, Tian L, Garcia SDO, Seposo X, Overcenco A, Zeka A, Goodman P, Dang TN, Dung DV, Mayvaneh F, Saldiva PHN, Williams G, Tong S (2017) Heat wave and mortality: A multicountry, multicommunity study. Environ Health Perspect 125:087006. https://doi.org/10.1289/EHP1026

Gutiérrez JM, Jones RG, Narisma GT, Alves LM, Amjad M, Gorodetskaya IV, Grose M, Klutse NAB, Krakovska S, Li J, Martínez-Castro D, Mearns LO, Mernild SH, Ngo-Duc T, van den Hurk B, Yoon J-H, (2021) Atlas. In Masson-Delmotte V, Zhai P, Pirani A, Connors SL, Péan C, Berger S, Caud N, Chen Y, Goldfarb L, Gomis MI, Huang M, Leitzell K, Lonnoy E, Matthews JBR, Maycock TK, Waterfield T, Yelekçi O, Yu R, Zhou B (eds) Climate Change 2021: The Physical Science Basis. Contribution of Working Group I to the Sixth Assessment Report of the Intergovernmental Panel on Climate Change. Available from http://interactiveatlas.ipcc.ch/. Accessed Sept 2023

Hagen I, Huggel C, Ramajo L, Chacón N, Ometto JP, Postigo JC, Castellanos EJ (2022) Climate change-related risks and adaptation potential in Central and South America during the 21st century. Environ Res Lett 17:033002. https://doi.org/10.1088/1748-9326/ac5271

Hancock PA, Vasmatzidis I (2003) Effects of heat stress on cognitive performance: the current state of knowledge. Int J Hyperth 19:355–372. https://doi.org/10.1080/0265673021000054630

He B-J, Wang J, Liu H, Ulpiani G (2021) Localized synergies between heat waves and urban heat islands: Implications on human thermal comfort and urban heat management. Environ Res 193:110584. https://doi.org/10.1016/j.envres.2020.110584

Henríquez C, Romero H (eds) (2019) Urban Climates in Latin America. Springer International Publishing, Cham. https://doi.org/10.1007/978-3-319-97013-4

Herold N, Alexander L, Green D, Donat M (2017) Greater increases in temperature extremes in low versus high income countries. Environ Res Lett 12:034007. https://doi.org/10.1088/1748-9326/aa5c43

Hersbach H, Bell B, Berrisford P, Hirahara S, Horányi A, Muñoz-Sabater J, Nicolas J, Peubey C, Radu R, Schepers D, Simmons A, Soci C, Abdalla S, Abellan X, Balsamo G, Bechtold P, Biavati G, Bidlot J, Bonavita M, Chiara G, Dahlgren P, Dee D, Diamantakis M, Dragani R, Flemming J, Forbes R, Fuentes M, Geer A, Haimberger L, Healy S, Hogan RJ, Hólm E, Janisková M, Keeley S, Laloyaux P, Lopez P, Lupu C, Radnoti G, Rosnay P, Rozum I, Vamborg F, Villaume S, Thépaut J (2020) The ERA5 global reanalysis. Q J R Meteorol Soc 146:1999–2049. https://doi.org/10.1002/qj.3803

Inostroza L, Baur R, Csaplovics E (2013) Urban sprawl and fragmentation in Latin America: A dynamic quantification and characterization of spatial patterns. J Environ Manage 115:87–97. https://doi.org/10.1016/j.jenvman.2012.11.007

Iturbide M, Fernández J, Gutiérrez JM, Bedia J, Cimadevilla E, Díez-Sierra J, Manzanas R, Casanueva A, Baño-Medina J, Milovac J, Herrera S, Cofiño AS, San Martín D, García-Díez M, Hauser M, Huard D, Yelekci Ö (2021) Repository supporting the implementation of FAIR principles in the IPCC-WG1 Atlas. Zenodo. https://doi.org/10.5281/zenodo.3691645. Available from:https://github.com/IPCC-WG1/Atlas. Accessed Sept 2023

Jendritzky G, Havenith G, Weihs P, Batchvarova E, DeDear R (2007) The universal thermal climate index UTCI goal and state of COST action 730. Environmental ergonomics XII. Biomed, Ljubljana, 509-512

Jendritzky G, De Dear R, Havenith G (2012) UTCI—Why another thermal index? Int J Biometeorol 56:421–428. https://doi.org/10.1007/s00484-011-0513-7

Jendritzky G (1990) Methodik zur räumlichen Bewertung der thermischen Komponente im Bioklima des Menschen: fortgeschriebenes Klima-Michel-Modell, Beiträge - Akademie für Raumforschung und Landesplanung (1988). Akademie für Raumforschung und Landesplanung, Hannover

Kántor N, Unger J (2011) The most problematic variable in the course of human-biometeorological comfort assessment — the mean radiant temperature. Open Geosciences 3:90–100. https://doi.org/10.2478/s13533-011-0010-x

Kendall MG (1975) Rank correlation methods, 4th edition. Charles Griffin, London

Kephart JL, Sánchez BN, Moore J, Schinasi LH, Bakhtsiyarava M, Ju Y, Gouveia N, Caiaffa WT, Dronova I, Arunachalam S, Diez Roux AV, Rodríguez DA (2022) City-level impact of extreme temperatures and mortality in Latin America. Nat Med 28:1700–1705. https://doi.org/10.1038/s41591-022-01872-6

Krüger EL (ed) (2021) Applications of the Universal Thermal Climate Index UTCI in Biometeorology: Latest Developments and Case Studies. Springer International Publishing, Cham. https://doi.org/10.1007/978-3-030-76716-7

Krüger EL, Silva TJV, Da Silveira Hirashima SQ, Da Cunha EG, Rosa LA (2021) Calibrating UTCI'S comfort assessment scale for three Brazilian cities with different climatic conditions. Int J Biometeorol 65:1463–1472. https://doi.org/10.1007/s00484-020-01897-x

Libonati R, Geirinhas JL, Silva PS, Monteiro Dos Santos D, Rodrigues JA, Russo A, Peres LF, Narizo L, Gomes MER, Rodrigues AP, DaCamara CC, Pereira JMC, Trigo RM (2022a) Drought–heatwave nexus in Brazil and related impacts on health and fires: A comprehensive review. Ann NY Acad Sci 1517:44–62. https://doi.org/10.1111/nyas.14887

Libonati R, Geirinhas JL, Silva PS, Russo A, Rodrigues JA, Belém LBC, Nogueira J, Roque FO, DaCamara CC, Nunes AMB, Marengo JA, Trigo RM (2022b) Assessing the role of compound drought and heatwave events on unprecedented 2020 wildfires in the Pantanal. Environ Res Lett 17:015005. https://doi.org/10.1088/1748-9326/ac462e

Liu W, Sun F, Feng Y, Li C, Chen J, Sang Y-F, Zhang Q (2021) Increasing population exposure to global warm-season concurrent dry and hot extremes under different warming levels. Environ Res Lett 16:094002. https://doi.org/10.1088/1748-9326/ac188f

Machado-Silva F, Libonati R, Melo De Lima TF, Bittencourt Peixoto R, De Almeida França JR, De Avelar Figueiredo Mafra Magalhães M, Lemos Maia Santos F, Abrantes Rodrigues J, DaCamara CC (2020) Drought and fires influence the respiratory diseases hospitalizations in the Amazon. Ecol Indic 109:105817. https://doi.org/10.1016/j.ecolind.2019.105817

Marengo JA, Ambrizzi T, Barreto N, Cunha AP, Ramos AM, Skansi M, Molina Carpio J, Salinas R (2022) The heat wave of October 2020 in central South America. Intl J Climatol 42:2281–2298. https://doi.org/10.1002/joc.7365

Menéndez CG, Giles J, Ruscica R, Zaninelli P, Coronato T, Falco M, Sörensson A, Fita L, Carril A, Li L (2019) Temperature variability and soil–atmosphere interaction in South America simulated by two regional climate models. Clim Dyn 53:2919–2930. https://doi.org/10.1007/s00382-019-04668-6

Meng Y, Hao Z, Feng S, Zhang X, Hao F (2022) Increase in compound dry-warm and wet-warm events under global warming in CMIP6 models. Glob Planet Change 210:103773. https://doi.org/10.1016/j.gloplacha.2022.103773

Mentaschi L, Duveiller G, Zulian G, Corbane C, Pesaresi M, Maes J, Stocchino A, Feyen L (2022) Global long-term mapping of surface temperature shows intensified intra-city urban heat island extremes. Glob Environ Change 72:102441. https://doi.org/10.1016/j.gloenvcha.2021.102441

Miranda VFVV, De Faria Peres L, José De Lucena A, França JRDA, Libonati R (2022) Urbanization-induced impacts on heat-energy fluxes in tropical South America from 1984 to 2020: The Metropolitan Area of Rio de Janeiro/Brazil. Build Environ 216:109008. https://doi.org/10.1016/j.buildenv.2022.109008

Mistry MN, Schneider R, Masselot P, Royé D, Armstrong B, Kyselý J, Orru H, Sera F, Tong S, Lavigne É, Urban A, Madureira J, García-León D, Ibarreta D, Ciscar J-C, Feyen L, De Schrijver E, De Sousa Zanotti Stagliorio Coelho M, Pascal M, Tobias A, Multi-Country Multi-City (MCC) Collaborative Research Network, Alahmad B, Abrutzky R, Saldiva PHN, Correa PM, Orteg NV, Kan H, Osorio S, Indermitte E, Jaakkola JJK, Ryti N, Schneider A, Huber V, Katsouyanni K, Analitis A, Entezari A, Mayvaneh F, Michelozzi P, de'Donato F, Hashizume M, Kim Y, Diaz MH, De La Cruz Valencia C, Overcenco A, Houthuijs D, Ameling C, Rao S, Seposo X, Nunes B, Holobaca I-H, Kim H, Lee W, Íñiguez C, Forsberg B, Åström C, Ragettli MS, Guo Y-LL, Chen B-Y, Colistro V, Zanobetti A, Schwartz J, Dang TN, Van Dung D, Guo Y, Vicedo-Cabrera AM, Gasparrini A (2022) Comparison of weather station and climate reanalysis data for modelling temperature-related mortality. Sci Rep 12:5178. https://doi.org/10.1038/s41598-022-09049-4

Mora C, Dousset B, Caldwell IR, Powell FE, Geronimo RC, Bielecki CR, Counsell CWW, Dietrich BS, Johnston ET, Louis LV, Lucas MP, McKenzie MM, Shea AG, Tseng H, Giambelluca TW, Leon LR, Hawkins E, Trauernicht C (2017) Global risk of deadly heat. Nature Clim Change 7:501–506. https://doi.org/10.1038/nclimate3322

Mukherjee S, Mishra AK, Ashfaq M, Kao S-C (2022) Relative effect of anthropogenic warming and natural climate variability to changes in Compound drought and heatwaves. J Hydrol 605:127396. https://doi.org/10.1016/j.jhydrol.2021.127396

Pappenberger F, Jendritzky G, Staiger H, Dutra E, Di Giuseppe F, Richardson DS, Cloke HL (2015) Global forecasting of thermal health hazards: the skill of probabilistic predictions of the Universal Thermal Climate Index (UTCI). Int J Biometeorol 59:311–323. https://doi.org/10.1007/s00484-014-0843-3

Patz JA, Campbell-Lendrum D, Holloway T, Foley JA (2005) Impact of regional climate change on human health. Nature 438:310–317. https://doi.org/10.1038/nature04188

Peel MC, Finlayson BL, McMahon TA (2007) Updated world map of the Köppen-Geiger climate classification. Hydrol Earth Syst Sci 11:1633–1644. https://doi.org/10.5194/hess-11-1633-2007

Peres LDF, Lucena AJD, Rotunno Filho OC, França JRDA (2018) The urban heat island in Rio de Janeiro, Brazil, in the last 30 years using remote sensing data. Int J Appl Earth Obs Geoinf 64:104–116. https://doi.org/10.1016/j.jag.2017.08.012

Perkins-Kirkpatrick SE, Lewis SC (2020) Increasing trends in regional heatwaves. Nat Commun 11:3357. https://doi.org/10.1038/s41467-020-16970-7

Power SB, Delage FPD (2019) Setting and smashing extreme temperature records over the coming century. Nat Clim Chang 9:529–534. https://doi.org/10.1038/s41558-019-0498-5

Qabbal L, Younsi Z, Naji H (2022) An indoor air quality and thermal comfort appraisal in a retrofitted university building via low-cost smart sensor. Indoor Built Environ 31:586–606. https://doi.org/10.1177/1420326X211015717

Regoto P, Dereczynski C, Chou SC, Bazzanela AC (2021) Observed changes in air temperature and precipitation extremes over Brazil. Int J Climatol 41:5125–5142. https://doi.org/10.1002/joc.7119

Romanello M, McGushin A, Di Napoli C, Drummond P, Hughes N, Jamart L, Kennard H, Lampard P, Solano Rodriguez B, Arnell N, Ayeb-Karlsson S, Belesova K, Cai W, Campbell-Lendrum D, Capstick S, Chambers J, Chu L, Ciampi L, Dalin C, Dasandi N, Dasgupta S, Davies M, Dominguez-Salas P, Dubrow R, Ebi KL, Eckelman M, Ekins P, Escobar LE, Georgeson L, Grace D, Graham H, Gunther SH, Hartinger S, He K, Heaviside C, Hess J, Hsu S-C, Jankin S, Jimenez MP, Kelman I, Kiesewetter G, Kinney PL, Kjellstrom T, Kniveton D, Lee JKW, Lemke B, Liu Y, Liu Z, Lott M, Lowe R, Martinez-Urtaza J, Maslin M, McAllister L, McMichael C, Mi Z, Milner J, Minor K, Mohajeri N, Moradi-Lakeh M, Morrissey K, Munzert S, Murray KA, Neville T, Nilsson M, Obradovich N, Sewe MO, Oreszczyn T, Otto M, Owfi F, Pearman O, Pencheon D, Rabbaniha M, Robinson E, Rocklöv J, Salas RN, Semenza JC, Sherman J, Shi L, Springmann M, Tabatabaei M, Taylor J, Trinanes J, Shumake-Guillemot J, Vu B, Wagner F, Wilkinson P, Winning M, Yglesias M, Zhang S, Gong P, Montgomery H, Costello A, Hamilton I (2021) The 2021 report of the Lancet Countdown on health and climate change: code red for a healthy future. Lancet 398:1619–1662. https://doi.org/10.1016/S0140-6736(21)01787-6

Romero-Lankao P, Qin H, Borbor-Cordova M (2013) Exploration of health risks related to air pollution and temperature in three Latin American cities. Soc Sci Med 83:110–118. https://doi.org/10.1016/j.socscimed.2013.01.009

Rusticucci M, Kyselý J, Almeira G, Lhotka O (2016) Long-term variability of heat waves in Argentina and recurrence probability of the severe 2008 heat wave in Buenos Aires. Theor Appl Climatol 124:679–689. https://doi.org/10.1007/s00704-015-1445-7

Seneviratne SI, Zhang X, Adnan M, Badi W, Dereczynski C, Di Luca A, Ghosh S, Iskandar I, Kossin J, Lewis S, Otto F, Pinto I, Satoh M, Vicente-Serrano SM, Wehner M, Zhou B (2021) Weather and climate extreme events in a changing climate. In Masson-Delmotte V, Zhai P, Pirani A, Connors SL, Péan C, Berger S, Caud N, Chen Y, Goldfarb L, Gomis MI, Huang M, Leitzell K, Lonnoy E, Matthews JBR, Maycock TK, Waterfield T, Yelekçi O, Yu R, Zhou B (eds) Climate Change 2021: The Physical Science Basis. Contribution of Working Group I to the Sixth Assessment Report of the Intergovernmental Panel on Climate Change. Cambridge University Press, Cambridge, United Kingdom and New York, NY, USA, pp. 1513–1766. https://doi.org/10.1017/9781009157896.013

Shaposhnikov D, Revich B, Bellander T, Bedada GB, Bottai M, Kharkova T, Kvasha E, Lezina E, Lind T, Semutnikova E, Pershagen G (2014) Mortality related to air pollution with the Moscow Heat Wave and Wildfire of 2010. Epidemiology 25:359–364. https://doi.org/10.1097/EDE.0000000000000090

Silva TJV, Hirashima SQS (2021) Predicting urban thermal comfort from calibrated UTCI assessment scale - A case study in Belo Horizonte city, southeastern Brazil. Urban Climate 36:100652. https://doi.org/10.1016/j.uclim.2020.100652

Souza DOD, Alvalá RCDS, Nascimento MGD (2016) Urbanization effects on the microclimate of Manaus: A modeling study. Atmos Res 167:237–248. https://doi.org/10.1016/j.atmosres.2015.08.016

Spennemann PC, Salvia M, Ruscica RC, Sörensson AA, Grings F, Karszenbaum H (2018) Land-atmosphere interaction patterns in southeastern South America using satellite products and climate models. Int J Appl Earth Obs Geoinf 64:96–103. https://doi.org/10.1016/j.jag.2017.08.016

United Nations (2022) World Population Prospects 2022: Summary of Results, Statistical Papers - United Nations (Ser. A), Population and Vital Statistics Report. United Nations. https://doi.org/10.18356/9789210014380

United Nations, Department of Economic and Social Affairs, Population Division (2019) World Urbanization Prospects: The 2018 Revision (ST/ESA/SER.A/420). United Nations, New York

Varghese BM, Barnett AG, Hansen AL, Bi P, Nairn J, Rowett S, Nitschke M, Hanson-Easey S, Heyworth JS, Sim MR, Pisaniello DL (2019) Characterising the impact of heatwaves on work-related injuries and illnesses in three Australian cities using a standard heatwave definition- Excess Heat Factor (EHF). J Expo Sci Environ Epidemiol 29:821–830. https://doi.org/10.1038/s41370-019-0138-1

Vicedo-Cabrera AM, Scovronick N, Sera F, Royé D, Schneider R, Tobias A, Astrom C, Guo Y, Honda Y, Hondula DM, Abrutzky R, Tong S, Coelho MDSZS, Saldiva PHN, Lavigne E, Correa PM, Ortega NV, Kan H, Osorio S, Kyselý J, Urban A, Orru H, Indermitte E, Jaakkola JJK, Ryti N, Pascal M, Schneider A, Katsouyanni K, Samoli E, Mayvaneh F, Entezari A, Goodman P, Zeka A, Michelozzi P, de'Donato F, Hashizume M, Alahmad B, Diaz MH, Valencia CDLC, Overcenco A, Houthuijs D, Ameling C, Rao S, Di Ruscio F, Carrasco-Escobar G, Seposo X, Silva S, Madureira J, Holobaca IH, Fratianni S, Acquaotta F, Kim H, Lee W, Iniguez C, Forsberg B, Ragettli MS, Guo YLL, Chen BY, Li S, Armstrong B, Aleman A, Zanobetti A, Schwartz J, Dang TN, Dung DV, Gillett N, Haines A, Mengel M, Huber V, Gasparrini A (2021) The burden of heat-related mortality attributable to recent human-induced climate change. Nat Clim Chang 11:492–500. https://doi.org/10.1038/s41558-021-01058-x

Vinogradova V (2021) Using the Universal Thermal Climate Index (UTCI) for the assessment of bioclimatic conditions in Russia. Int J Biometeorol 65:1473–1483. https://doi.org/10.1007/s00484-020-01901-4

Wang XL Swail VR (2001) Changes in extreme wave heights in northern hemisphere oceans and related atmospheric circulation regimes. J Clim 14:2204–2221

Wellenius GA, Eliot MN, Bush KF, Holt D, Lincoln RA, Smith AE, Gold J (2017) Heat-related morbidity and mortality in New England: evidence for local policy. Environ Res 156:845–853. https://doi.org/10.1016/j.envres.2017.02.005

World Meteorological Organization (2017) WMO Guidelines on the Calculation of Climate Normals. https://library.wmo.int/idurl/4/55797

Wu Y, Wen B, Li S, Gasparrini A, Tong S, Overcenco A, Urban A, Schneider A, Entezari A, Vicedo-Cabrera AM, Zanobetti A, Analitis A, Zeka A, Tobias A, Alahmad B, Armstrong B, Forsberg B, Íñiguez C, Ameling C, De La Cruz Valencia C, Åström C, Houthuijs D, Van Dung D, Royé D, Indermitte E, Lavigne E, Mayvaneh F, Acquaotta F, de'Donato F, Sera F, Carrasco-Escobar G, Kan H, Orru H, Kim H, Holobaca I-H, Kyselý J, Madureira J, Schwartz J, Katsouyanni K, Hurtado-Diaz M, Ragettli MS, Hashizume M, Pascal M, De Sousa Zanotti Stagliorio Coélho M, Scovronick N, Michelozzi P, Goodman P, Nascimento Saldiva PH, Abrutzky R, Osorio S, Dang TN, Colistro V, Huber V, Lee W, Seposo X, Honda Y, Bell ML, Guo Y (2022) Fluctuating temperature modifies heat-mortality association around the globe. Innovation 3:100225. https://doi.org/10.1016/j.xinn.2022.100225

Xu C, Kohler TA, Lenton TM, Svenning J-C, Scheffer M (2020) Future of the human climate niche. Proc Natl Acad Sci USA 117:11350–11355. https://doi.org/10.1073/pnas.1910114117

Zeng D, Wu J, Mu Y, Deng M, Wei Y, Sun W (2020) Spatial-temporal pattern changes of UTCI in the China-Pakistan economic Corridor in recent 40 years. Atmosphere 11:858. https://doi.org/10.3390/atmos11080858

Zhang Y, Li Q, Ge Y, Du X, Wang H (2022) Growing prevalence of heat over cold extremes with overall milder extremes and multiple successive events. Commun Earth Environ 3:73. https://doi.org/10.1038/s43247-022-00404-x